Biosensors and Bioelectronics 25 (2010) 2356–2360

Contents lists available at ScienceDirect

Biosensors and Bioelectronics

journal homepage: www.elsevier.com/locate/bios

A nonenzymatic cholesterol sensor constructed by using porous tubular silver nanoparticles

Yanfen Li, Hongyan Bai, Qian Liu, Jianchun Bao, Min Han, Zhihui Dai*

Jiangsu Key Laboratory of Biofunctional Materials, College of Chemistry and Environmental Science, Nanjing Normal University, Nanjing, 210097, China

ARTICLE INFO

Article history:
Received 27 January 2010
Received in revised form 23 March 2010
Accepted 28 March 2010
Available online 3 April 2010

Keywords:
Nonenzymatic sensor
Cholesterol
Porous tubular Ag nanoparticles
Electrodeposition

ABSTRACT

Porous tubular silver (Ag) nanoparticles were successfully synthesized by electrodeposition of Ag into cadmium sulfide (CdS) modified porous anodic alumina (PAA) template and removal of CdS subsequently. Only the solid nanorods were obtained without CdS. The strong affinity between S^{2-} and Ag (I) caused preferential deposition of Ag on the pore walls to form tubular Ag. After removal of CdS, porous tubular Ag nanoparticles were obtained. This novel nanostructure was characterized by XRD, TEM, FESEM, EDS and nitrogen adsorption–desorption isotherms. Using porous tubular Ag nanoparticles modified glassy carbon electrode (GCE) as a working electrode, a good nonenzymatic cholesterol sensor was constructed, which showed markedly improved electrocatalytic activity toward cholesterol oxidation compared to that of solid Ag nanorods. Under optimal detection conditions, the constructed sensor had a linear response range of 2.8×10^{-4} M to 3.3×10^{-2} M and the detection limit was 1.8×10^{-4} M at a signal-to-noise ratio of 3. The biosensor showed an acceptable reproducibility, good stability and low interferences. To the best of our knowledge, it is the first example of a nonenzymatic cholesterol biosensor based on Ag nanoparticles. The experimental results demonstrated that porous tubular Ag nanoparticles provided a promising platform for rational design and fabrication of nonenzymatic cholesterol sensors.

1. Introduction

The detection of cholesterol has been paid more and more attention in biomedical fields and plays an increasingly important role in the improving life quality (Rakow and Suslick, 2000; Arya et al., 2007). Abnormalities of cholesterol levels are symptoms of several diseases, such as hypertension, coronary heart disease, arteriosclerosis, brain thrombosis, lipid metabolism dysfunction and myocardial infarction (Aravamudhan et al., 2007). Various methods have been reported for the analysis of cholesterol in serum including colorimetric (Qureshi et al., 2009) spectrophotometric (Pires et al., 2003), high performance liquid chromatography (HPLC) (Canabate-Diaz et al., 2007) and electrochemical methods (Hosokawa et al., 2009; Barbadillo et al., 2009). Among them, some methods often present certain disadvantages, such as lack of specificity and selectivity due to interfering reactions and use of unstable and corrosive reagents (Brahim et al., 2001). Amperometric biosensors based on electron transfer between an electrode and immobilized cholesterol oxidase are especially promising because of their practical advantages such as operational simplicity, low fabrication cost and suitable for real time detection (Clark and Lyons, 1962; Updike and Hicks, 1967; Yu et al., 2003). Although the enzyme-based sensor shows high selectivity and excellent sensitivity, the activity of enzyme decreases with the use of the sensor and the enzyme is easily denatured during its immobilization procedure due to the intrinsic nature of enzyme. In addition, the activity of enzyme is prone to be affected by temperature, pH, humidity, and toxic chemicals. Furthermore, the reproducibility of enzyme-based sensor is not satisfactory and needs to be further improved (Park et al., 2006). These disadvantages restrict the application of cholesterol biosensor.

In order to overcome the drawbacks of enzymatic cholesterol sensors, recently, nonenzymatic cholesterol sensors have been designed and fabricated (Ricci and Palleschi, 2005; Yi et al., 2009). The porous Pt nanostructure has been proved to be an ideal candidate for the fabrication of nonenzymatic cholesterol sensors (Yi et al., 2009). In addition, cholesterol sensor based on the Prussian blue modified electrode which can catalyze the reduction of hydrogen peroxide has been fabricated (Ricci and Palleschi, 2005). However, porous tubular metal nanostructure, which possesses porous exterior (wall) and hollow interior, has not been effectively used for the fabrication of nonenzymatic cholesterol sensors. Therefore, synthesizing porous tubular metal nanoparticles and fabricating nonenzymatic cholesterol sensor become an interesting topic.

In recent years, there has been much interest in the fabrication of one-dimensional (1D) nanostructure arrays with well controllable microstructure because of their potential utilization in nanode-

* Corresponding author. Tel.: +86 25 83598280.
E-mail address: daizhihuii@njnu.edu.cn (Z. Dai).

0956-5663/$ – see front matter © 2010 Elsevier B.V. All rights reserved.
doi:10.1016/j.bios.2010.03.036

vices (Che et al., 1998; Huang et al., 2001; Tang et al., 2001; Kohli et al., 2004). One likely major application for 1D nanostructure array is to fabricate chemical sensors (Kolmakov et al., 2003; Heins et al., 2005). The extremely high surface-to-volume ratios associated with these nanostructures make their electrical properties extremely sensitive to species adsorbed on surfaces and result in excellent sensitivity (Zhang et al., 2009).

As far as we know, there are few reports on the sensing application of porous tubular nanostructure. Here, we report the synthesis of porous tubular Ag nanoparticles and its application in nonenzymatic cholesterol sensor. Porous tubular Ag nanoparticles was synthesized by a simple method, i.e. the PAA template was firstly pretreated with cadmium sulfide (CdS) by the reaction of Cd^{2+} with S^{2-}, and then Ag was electrodeposited within the modified PAA to obtain the CdS-containing Ag nanotube. After removal of CdS, porous tubular Ag was obtained. The reason why we chose CdS as a pretreated agent was that the strong affinity between S^{2-} and Ag(I) could cause preferential deposition of Ag on the pore walls to form tubular Ag. Using the obtained porous tubular Ag nanoparticles as an active material to modify glassy carbon electrode (GCE), a good nonenzymatic cholesterol sensor was constructed, which indicated that the porous tubular Ag nanoparticles were promising in fabrication of nonenzymatic cholesterol sensors.

2. Experimental section

2.1. Reagents

Cholesterol, uric acid (UA), glucose, glycerol and β-estradiol were purchased from Sigma and used as received. Serum samples were provided by Jiangsu Institute of Cancer Prevention and Cure and they were obtained by centrifugation of blood for about 5 min with the rotation rate of 3000–4000 rpm/min. PAA membranes with the pore sizes of 20 nm and 100 nm were from Whatman Corporation. The quoted pore diameters of the PAA membranes were 20 nm and 100 nm, but actually, according to the SEM image of the PAA membrane, there was a pore diameter distribution mainly in the range of 40–60 nm and 150–220 nm, respectively (Bao et al., 2002). Chitosan was purchased from Shanghai Sinopharm Chemical Reagent Co. Ltd. Ammonia solution (25%) was purchased from Nanjing chemical reagent No. 1 factory. Silver nitrate ($AgNO_3$) was purchased from Shanghai Chemical Reagent Co. All other chemicals were of analytical grade and were used without further purification. All solutions were made up with doubly distilled water.

2.2. Preparation of porous tubular Ag nanoparticles and their colloidal solutions

Fig. 1 shows a scheme of the suction equipment. Two overlapped PAA templates were placed in the groove of teflon. The upper PAA template was with pore size of 100 nm and the bottom was with pore size of 20 nm. 0.1 M of $CdCl_2$ was firstly introduced to the pores of PAA templates by a slight suction method, and then injecting 0.1 M of Na_2S solution. CdS was deposited on the pore wall of the PAA template by the reaction of Cd^{2+} and S^{2-}. After that, the upper template was taken out, washed with doubly distilled water and allowed to dry under ambient conditions. The PAA template displayed yellow which indicated CdS intercalating the pores of PAA. Then, a thin Au layer was evaporated on one side of the PAA membrane as a working electrode. The template was then immersed into a mixture of 0.01 M of $AgNO_3$ and 0.01 M ammonia solution followed by adding 0.45 g H_3BO_3. Electrodeposition was carried out in a three-electrode electrochemical cell with the bare side of the PAA membrane facing upward and the deposition solution confined to the bare side of the PAA membrane, a platinum wire as the counter electrode and a saturated calomel electrode as a reference electrode. The electrodeposition proceeded in a constant current mode with a typical deposition current density of 0.7 mA cm^{-2} for 2 h. After the deposition, the PAA template was dissolved by 2.0 M of NaOH solution. 2.0 M of HCl solution was used to further dissolve CdS. For comparison, the electrochemical deposition of Ag without CdS pre-deposition was also employed.

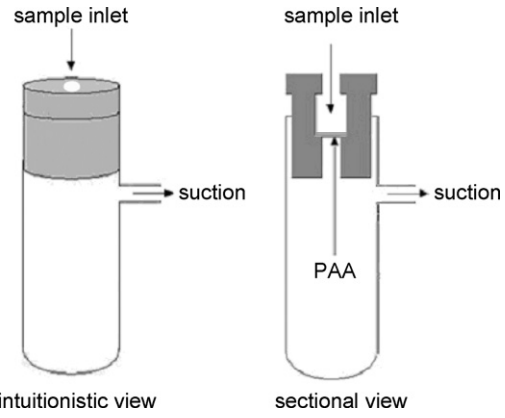

Fig. 1. Scheme of the suction equipment. PAA: two overlapped PAA templates with the upper of pore size of 100 nm and the bottom of 20 nm.

2.3. Electrode modification

The GCE (3 mm in diameter) were polished to a mirror-like finish with 1.0 μm, 0.3 μm and 0.05 μm alumina slurry (Beuhler) followed by rinsing thoroughly with doubly distilled water. The electrodes were successively sonicated in 1:1 nitric acid, acetone and doubly distilled water, and then allowed to dry at room temperature. 0.45 mg 1D porous Ag nanoparticles were dispersed into 0.1 mL water to obtain a suspension of 4.5 mg mL^{-1} 1D porous Ag nanoparticles. 1.5 μL of suspension and 2.5 μL of 3% chitosan solution of acetic acid/water (V:V, 1:100) were successively dispersed on GCE surface, and allowed to dry under ambient condition for 3 h. After the modified electrode was rinsed with doubly distilled water twice or thrice, the 1D porous Ag nanoparticles modified GCE was obtained.

2.4. Apparatus and measurements

Phase characterization was performed by means of X-ray diffraction (XRD) using a D/Max-RA diffractometer with Cu Kα radiation. The morphology and particle sizes of the samples were characterized by JEM-200CX transmission electron microscope (TEM) working at 200 kV. A small amount of the yellow sample was dispersed in ethanol, and then a drop of this solution was deposited on a carbon-coated copper grid for TEM observation. Energy dispersive spectrum (EDS) was performed with a PV9100 scanning electron microanalyzer. Nitrogen adsorption–desorption isotherms were obtained using an ASAP 2000 instrument (Micromeritics. Norcross, GA). Cyclic voltammetric and amperometric measurements were performed on CHI 660B electrochemical workstation (CH Instruments, USA). All electrochemical experiments were carried out in a cell containing 5.0 mL of certain concentration of NaOH at room temperature (25 ± 2 °C) and using the modified electrode as a working electrode. The amperometric experiments were carried out by applying a potential of 0.35 V on a stirred cell. The sensor responses were measured as the difference between total and residual currents.

3. Results and discussion

3.1. Characterization of porous tubular Ag nanoparticles

Supplementary Fig. S1 shows XRD pattern of the Ag nanoparticles prepared by the electrodeposition using PAA membrane pre-deposited with CdS as a template. The diffraction peaks in the range of $5 < \theta < 85^\circ$ can be indexed as cubic Ag (1 1 1), (2 0 0), (2 2 0) and (3 1 1) (2 2 2) and the lattice parameter is $a = 4.0929$ Å, which all are in good accordance with the values on the standard card (JCAGS 4-0783). It should be mentioned that the diffraction peaks of the CdS are not observed in XRD pattern, which might result from the little amount in the sample.

Fig. 2A shows the TEM image of the sample after removal of the PAA. It can be seen that the Ag nanoparticles are of the pale colour regions in the central parts in contrast to dark edges, implying a tubular structure. The average diameter of the tubes is about 200 nm, which is identical to the actual pore diameter of the PAA template (Bao et al., 2002). In order to confirm the components, EDS analysis is performed (Fig. 2B). It shows that the sample is composed of Ag, Cd and S. Fig. 2C shows the TEM image of the tubular Ag nanoparticles after removal of the PAA membrane and CdS. It displays that the tubular wall is made of many aggregated nanoparticles and there are many holes on the tubular wall. Corresponding EDS analysis (Fig. 2D) shows no existence of S and Cd atoms, indicating the CdS has been removed completely. If the electrodeposition is conducted without the use of CdS and keeps other conditions constant, only solid Ag nanorods are obtained (Fig. 2E). We think that the strong affinity of S^{2-} for Ag causes preferential deposition of Ag on the tubular walls to form Ag nanotubes when Ag is electrodeposited into the pores.

3.2. Electrocatalytic oxidation of cholesterol

Cyclic voltammograms (CVs) of 1D porous tubular Ag nanoparticles modified GCE in the absence and presence of 7.4 mM cholesterol in 0.1 M NaOH were shown in Fig. 3, respectively. In contrast, CVs of bare GCE in the absence and presence of 7.4 mM cholesterol in 0.1 M NaOH were also shown in inset in Fig. 3, respectively. Upon addition of cholesterol to the solution, the shape of CV for 1D porous Ag nanoparticles changed dramatically with an increase of oxidation current, displaying an obvious electrocatalytic

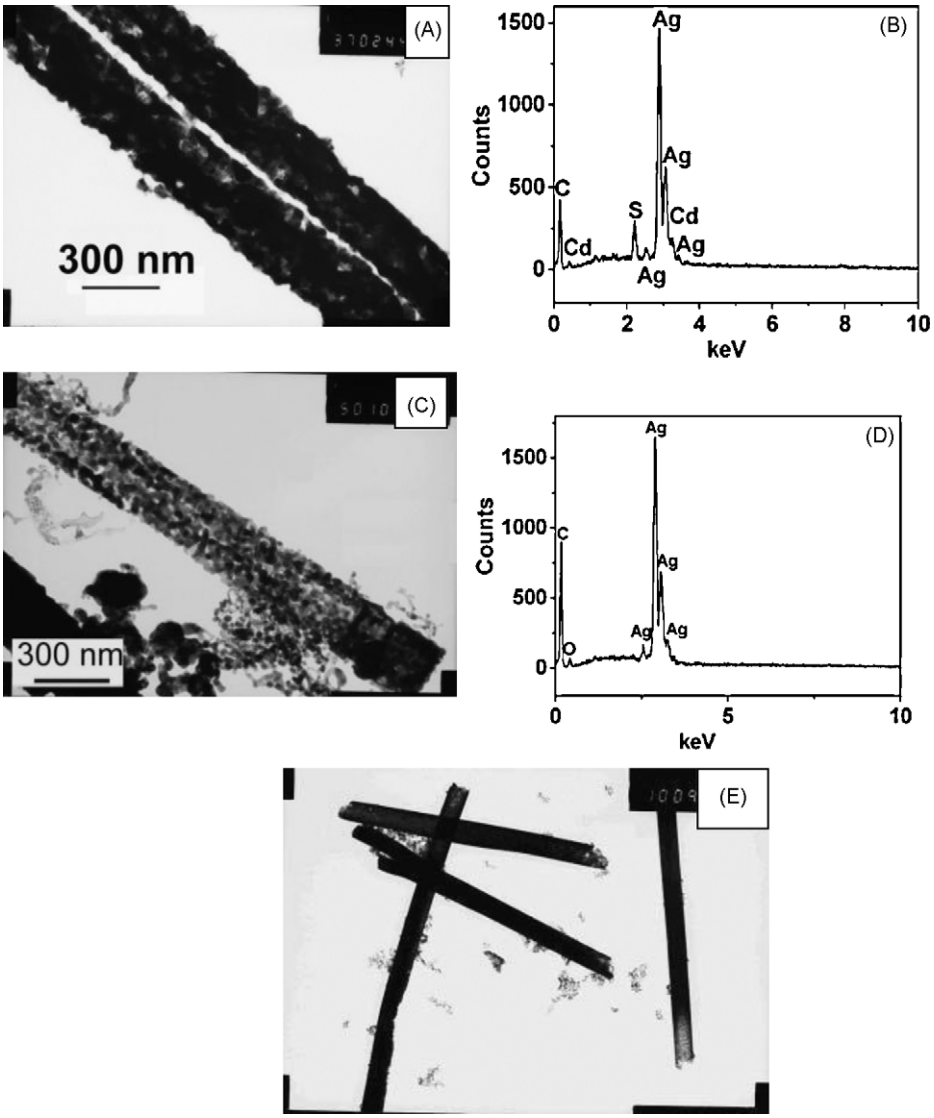

Fig. 2. TEM (A) image of tubular Ag nanoparticles by using PAA as a template via pre-deposition of CdS after removal of the PAA membrance. EDS pattern (B) of the sample in panel (A). TEM (C) image of tubular Ag nanoparticles after removal of the PAA membrane and CdS. EDS pattern (D) of the sample in panel (C). Electrodeposition current: 0.7 mA cm^{-2}; electrodeposition time: 2 h.

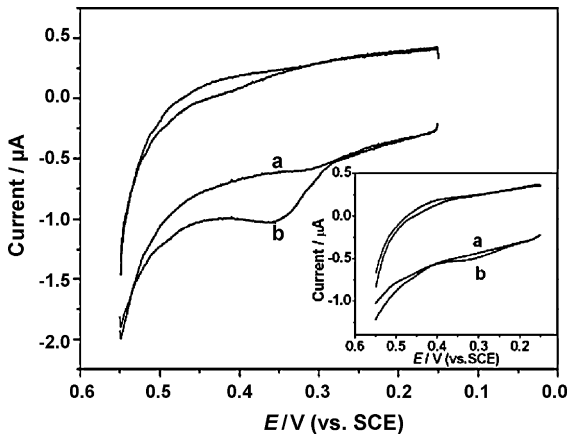

Fig. 3. Cyclic voltammograms of bare GCE (inset) and 1D porous Ag nanoparticles modified GCE in the absence (a) and presence (b) of 7.4 mM cholesterol in 0.1 M NaOH at 100 mV s^{-1}.

behavior to the oxidation of cholesterol. Almost no electrocatalytic current was observable at a bare GCE when cholesterol was added to 0.1 M NaOH. Thus, 1D porous Ag nanoparticles modified GCE showed an electrocatalytic response to the reduction of cholesterol.

Supplementary Fig. S2 shows CVs of 1D porous Ag nanoparticles modified GCE in 0.1 M NaOH solution without (curve a) and with 4.0 mM (curve b), 4.8 mM (curve c), 5.7 mM (curve d), 6.5 mM (curve e) and 7.4 mM (curve f) cholesterol at a scan rate of 100 mV s^{-1}. It is noted that upon addition of cholesterol, 1D porous Ag nanoparticles modified GCE exhibits an increase at about +0.35 V. Furthermore, with increasing cholesterol concentration the response increased which indicated nonenzymatic cholesterol sensor could be constructed based on the electrocatalytic oxidation of cholesterol on 1D porous Ag nanoparticles.

The amperometric responses of the solid Ag nanowires and porous tubular Ag modified GCEs upon additions of 5.0 μL 2.5 M cholesterol to 5 mL 0.1 M NaOH solution at an applied potential of +0.35 V were shown in Fig. 4, respectively. It can be seen that the solid Ag nanorods modified GCE showed a much smaller response to cholesterol than that of porous tubular Ag modified GCE at the same cholesterol concentration. It might result from the different surface areas of the porous tubular Ag and Ag solid nanorods. The BET surface area of the porous tubular Ag nanoparticles was about 55.4 m^2 g^{-1}, which was much larger than the value of about 10.0 m^2 g^{-1} calculated for the surface of solid Ag nanorods. Therefore, we have chosen the porous tubular Ag nanoparticles as the materials for constructing nonenzymatic cholesterol sensor.

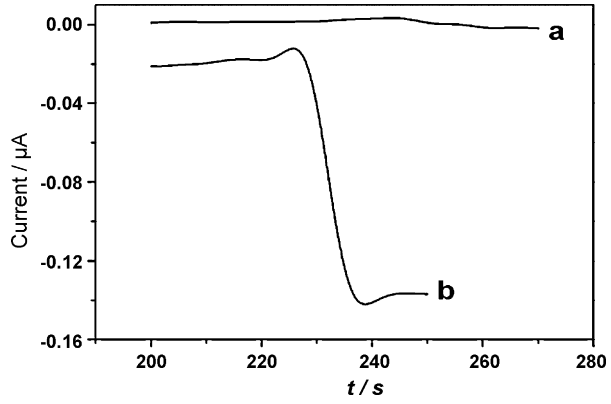

Fig. 4. Amperometric responses of solid Ag nanowire (a) and 1D porous tubular Ag (b) modified GCEs at +0.35 V upon addition of 5.0 μL 2.5 M cholesterol to 5.0 mL 0.1 M NaOH.

3.3. Optimization conditions for the sensor

Various factors influencing the response of the sensor were investigated in order to improve the performance of the sensor, such as pHs of solutions, the applied potential and the amount of Ag nanoparticles covered on the surface of the working electrode. The influence of pH on the response current of the sensor was illustrated in Supplementary Fig. S3A. With the increase of pH value, the response currents of the oxidation of cholesterol increased because cholesterol is more easily oxidized at high pH. When the pH was 13, the response current reached the maximum. The effect of the applied potential on the response current of the oxidation of cholesterol was illustrated in Supplementary Fig. S3B. When the applied potential increased from +0.2 V to +0.45 V, the maximum response current was observed at +0.35 V. The influence of the amount of the Ag nanoparticles covered on the surface of electrode was illustrated in Supplementary Fig. S3C. It showed that the response current of the oxidation of cholesterol was the highest when the amount of Ag nanoparticles was 1.5 μL (concentration: 4.5 mg mL^{-1}). When the electrode was prepared with 1.5 μL or less than 1.5 μL of Ag nanoparticles, the current of the electrode was small because the amount was less and the sensor could not reach the maximal response. While the electrode was prepared with 1.5 μL or more than 1.5 μL of Ag nanoparticles, the current of the electrode became small. The possible reason might be that the membrane of the modified electrode was thick, inhibiting the diffusion of cholesterol to the electrode surface. Therefore, 0.1 M pH 13 NaOH, at 0.35 V and 1.5 μL Ag nanoparticles covered on the surface of the working electrode were chosen as the detection solution of cholesterol.

3.4. Amperometric response and calibration curve

Fig. 5 showed a typical current–time plot for the sensor at on successive addition of 5.0 μL 0.28 M cholesterol to 5.0 mL 0.1 M NaOH at 0.35 V. When an aliquot of cholesterol was added into the buffer solution, the oxidation current rose steeply to reach a stable value. The sensor achieved 95% of steady-state current in less than 20 s. Such a short response time indicated a fast electron exchange between porous tubular Ag and cholesterol.

The calibration curve of the sensor under the optimized conditions showed a linear range from 2.8×10^{-4} M to 3.3×10^{-2} M for cholesterol with a correlation coefficient of 0.9988 ($n = 20$) and the

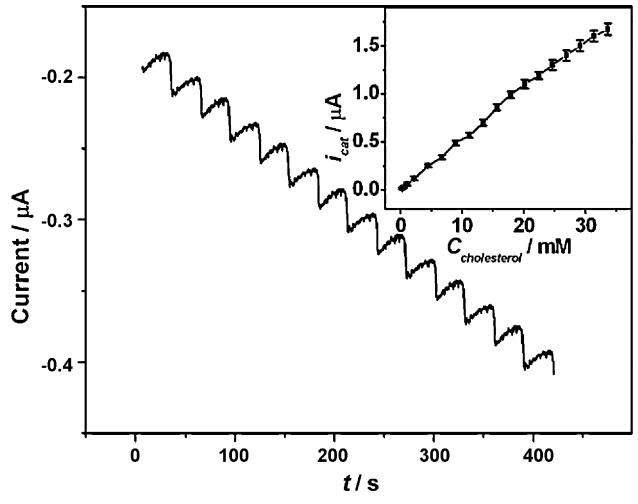

Fig. 5. Amperometric responses of 1D porous tubular Ag modified GCE at 0.35 V upon successive additions of 5.0 μL 0.28 M cholesterol to 5.0 mL 0.1 M pH 13 NaOH. Inset: plot of catalytic current *vs* cholesterol concentration (RSD: 4.51%).

Table 1
Determination of cholesterol concentrations in the blood sample.

Sample no.	Measured by the biosensor		Measured by HPLC	
	Concentrations/mM	RSD/%	Concentrations/mM	RSD/%
1	4.20	3.31	4.48	3.76
2	3.12	2.88	3.25	3.48
3	2.43	3.34	2.13	2.77
4	1.56	2.35	1.66	3.85
5	1.21	3.44	1.38	3.16

It is an average value of the response of five measurements for each sample.

detection limit of 1.8×10^{-4} M at 3σ. The linear range was wider than 10–400 mg/dL for a cholesterol biosensor based on metal oxide-chitosan nanocomposite (Malhotra and Kaushik, 2009) and 5–400 mg/dL for a cholesterol biosensor based on electrochemically prepared polyaniline conducting polymer film in presence of a nonionic surfactant (Khan et al., 2009). The limit of detection was much lower than 5 mg/dL from Malhotra et al. and Khan et al.

The Ag nanotubes modified electrode in our protocol had good stability. After more than 50 successive measurements the response retained 95.3% of its initial activity. The good stability might result from Ag oxidized to Ag^+ and then to form Ag_2O in an alkaline solution (Tominaga et al., 2006). Due to the enzyme-free sensor, porous tubular Ag membrane imparted the sensor a good long-term stability. The sensor could retain 93% of its initial activity to cholesterol within a storage period of 60 days in 0.1 M NaOH, while 89% of activity to cholesterol was retained when stored in air. The fabrication reproducibility of six electrodes, made independently, showed an acceptable reproducibility with RSD of 5.1% for the currents determined at a cholesterol concentration of 10 mM.

3.5. Interferences

Cholesterol is an important component in biological samples. Some species that possibly interfered with cholesterol determination were also studied (Supplementary Fig. S4). It was found that 10 times of glucose and uric acid had almost no interference with the determination of cholesterol. When the concentrations of glycerol and β-estradiol were up to 10 times higher than that of cholesterol, it also almost did not affect the detection of cholesterol (less than 6.2%) which might be resulted from the different structures.

3.6. Real sample detection

To evaluate its applicability, the electrode was used for the detection of the concentration of cholesterol in blood sample. The recovery measurements were first carried out. The recoveries for the assay of 1.0–5.0 mM cholesterol were between 95.7 and 105.1% for five detections, indicating the developed electrode had high accuracy in measuring the blood cholesterol.

Five blood samples were analyzed using five independently prepared electrodes. The determined results were compared with those measured with HPLC (Table 1). It was shown that the values measured by the developed biosensor were in good agreement with the data from HPLC, indicating that the cholesterol biosensor had great potential for practical application for the analysis of cholesterol in real clinical samples.

4. Conclusions

This work provided the first example of an Ag based nonenzymatic cholesterol biosensor. The electrooxidation of cholesterol at a porous tubular Ag modified electrode was studied. The porous tubular Ag nanoparticles were successfully synthesized by a simple method: pre-deposition of CdS into the pores of PAA template followed by electrodeposition of Ag and then removal of CdS. Current experimental results demonstrated that porous tubular Ag nanoparticles possessed a higher electrocatalytic activity toward cholesterol oxidation for cholesterol detection than that of solid nanorods. The sensor showed a wide linear range, low detection limit, good reproducibility and stability. Such a novel porous tubular nanostructure provided good opportunities for rational design and fabrication of high efficient and stable nonenzymatic biosensors.

Acknowledgements

This work was supported by the National Natural Science Foundation of China (Nos. 20875046, 20871070 and 20901041).

Appendix A. Supplementary data

Supplementary data associated with this article can be found, in the online version, at doi:10.1016/j.bios.2010.03.036.

References

Aravamudhan, S., Ramgir, N.S., Bhansali, S., 2007. Sens. Actuators B 127, 29–35.
Arya, S.K., Solanki, P.R., Singh, S.P., Kaneto, K., Pandey, M.K., Datta, M., Malhotra, B.D., 2007. Biosens. Bioelectron. 22, 2516–2524.
Bao, J.C., Xu, D.P., Zhou, Q.F., Xu, Z., Feng, Y.Y., Zhou, Y.M., 2002. Chem. Mater. 14, 4709–4713.
Barbadillo, M., Casero, E., Petit-Dominguez, M.D., Vazquez, L., Pariente, F., Lorenzo, E., 2009. Talanta 80, 797–802.
Brahim, S., Narinesingh, D., Guiseppi-Elie, A., 2001. Anal. Chim. Acta 448, 27–36.
Canabate-Diaz, B., Segura, C.A., Fernandez-Gutierrez, A., Belmonte, V.A., Garrido, F.A., Martinez, V.J.L., Duran, M.J., 2007. Food Chem 102, 593–598.
Che, G.L., Lakshmi, B.B., Fisher, E.R., Martin, C.R., 1998. Nature 393, 346–349.
Clark, L.C., Lyons, C., 1962. Ann. N.Y. Acad. Sci. 102, 29–45.
Heins, E.A., Siwy, Z.S., Baker, L.A., Martin, C.R., 2005. Nano Lett. 5, 1824–1829.
Hosokawa, Y.Y., Hakamata, H., Murakami, T., Aoyagi, S., Kuroda, M., Mimaki, Y., Ito, A., Morosawa, S., Kusu, F., 2009. Electrochim. Acta 54, 6412–6416.
Huang, M.H., Mao, S., Feick, H., Yan, H.Q., Wu, Y.Y., Kind, H., Weber, E., Russo, R., Yang, P.D., 2001. Science 292, 1897–1899.
Khan, R., Solanki, P.R., Kaushik, A., Singh, S.P., Ahmad, S., Malhotra, B.D., 2009. J. Polym. Res. 16, 363–373.
Kohli, P., Harrell, C.C., Cao, Z.H., Gasparc, R., Tan, W.H., Martin, C.R., 2004. Science 305, 984–986.
Kolmakov, A., Zhang, Y.X., Cheng, G.S., Moskovits, M., 2003. Adv. Mater. 15, 997–1000.
Malhotra, B.D., Kaushik, A., 2009. Thin Solid Films 518, 614–620.
Park, S., Boo, H., Chung, T.D., 2006. Anal. Chim. Acta 556, 46–57.
Pires, C.K., Reis, B.F., Galhardo, C.X., Martelli, P.B., 2003. Anal. Lett. 36, 3011–3024.
Qureshi, R.N., Kok, W.T., Schoenmakers, P.J., 2009. Anal. Chim. Acta 654, 85–91.
Rakow, N.A., Suslick, K.S., 2000. Nature 406, 710–713.
Ricci, F., Palleschi, G., 2005. Biosens. Bioelectron. 21, 389–407.
Tang, Z.K., Zhang, L.Y., Wang, N., Zhang, X.X., Wen, G.H., Li, G.D., Wang, J.N., Chan, C.T., Sheng, P., 2001. Science 292, 2462–2465.
Tominaga, M., Shimazoe, T., Nagashima, M., Kusuda, H., Kubo, A., Kuwahara, Y., Taniguchi, I., 2006. J. Electroanal. Chem. 590, 37–46.
Updike, S.J., Hicks, G.P., 1967. Nature 214, 986–988.
Yi, J.L., Jung, D.K., Jae, Y.P., 2009. J. Korean Phys. Soc. 54, 1769–1773.
Yu, J.H., Liu, S.Q., Ju, H.X., 2003. Biosens. Bioelectron. 19, 401–409.
Zhang, X.Y., Lu, W., Da, J.Y., Wang, H.T., Zhao, D.Y., Webley, P.A., 2009. Chem. Commun., 195–197.